

# Synthesis, Characterization and In-Vitro Antibacterial Propriety of Cu(II), Co(II) and Bi(III) Complexes with (Z)-1-(2-Phenylhydrazono) Naphthalen-2(1H)-one as a Ligand

Emmanuel F. Sopbué<sup>1,\*</sup>, Raoul K. Dennue<sup>1</sup>, Jean-de-Dieu Tamokou<sup>2</sup>, Apollinaire Tsopmo<sup>3</sup>, Giscard Doungmo<sup>4</sup>, Peter F. W. Simon<sup>5</sup>, Bruno N. Lenta<sup>6</sup>, Jules R. Kuate<sup>2</sup>

<sup>1</sup>Laboratory of Applied Synthetic Organic Chemistry, Department of Chemistry, Faculty of Science, University of Dschang, Dschang, Republic of Cameroon

<sup>2</sup>Research Unit of Microbiology and Antimicrobial Substances, Department of Biochemistry, Faculty of Science, University of Dschang, Dschang, Republic of Cameroon

<sup>3</sup>Department of Chemistry, Carleton University, Colonel By Drive K1S 5B6, Ottawa, Canada

<sup>4</sup>Institut für Anorganische Chemie, Christian-Albrechts-Universität zu Kiel, Max-Eyth-Str. 2, 24118 Kiel, Germany

<sup>5</sup>Polymer Chemistry Laboratory, Faculty of Life Sciences, Rhine-Waal University of Applied Sciences, Campus Kleve, Marie-Curie Strasse 1, D-47533 Kleve, Germany

<sup>6</sup>Higher Teacher's Training College, University of Yaounde I, Yaounde, Cameroon

**Abstract** The present work deals with the synthesis, characterization and antibacterial evaluation activity of new transition metals complexes obtained from the reaction of  $\text{CoC}_2\text{O}_4 \cdot 2\text{H}_2\text{O}$ ,  $\text{CuCl}_2 \cdot 2\text{H}_2\text{O}$  and  $\text{BiCl}_3$  with 1-(2-phenylhydrazono) naphthalen-2-one used as ligand. The structures of the ligand and its complexes were assigned on the basis of the available spectroscopic (IR, UV, 1&2D NMR, powder XRD), spectrometric (ESI-MS) and elemental analyses data. In-vitro antibacterial activity of the synthesized compounds have been screened against gram positive and gram-negative bacteria by using microdilution method. The antibacterial activity assay results showed that metal complexes (CMI = 32-128  $\mu\text{g}/\text{mL}$ ) possess higher antibacterial activity compared to the free ligand (CMI = 64-128  $\mu\text{g}/\text{mL}$ ).

**Keywords** Synthesis, Hydrazone ligand, Chelate complexes, Antibacterial activity

## 1. Introduction

During the last decade azo compounds are well known for their wide use in the dyeing of textile fibers and coloring of different materials, e. g. for plastics, biological as well as medical studies. Furthermore, they are also well established for advanced applications in organic synthesis and high technology areas such as laser, liquid crystalline displays, electro-optical devices and ink-jet printers [1,2]. Therefore, a large number of (N, O)-donor ligands in azo imine family have been prepared [3,4] and used to form very stable chelate complexes with various applications such as optical data storage [5], photo switching, nonlinear optics and photochromic materials, dyes, chemical analysis [6,7], and pharmaceuticals [8]. Both azo dyes and their metal complexes play an essential role in the chemistry of living organisms and their

biological importance continues to be studied [9]. Although a rapid and convenient synthesis of azo dyes ligands and their metal complexes have already been described, the UV-visible spectral behavior in different pH regimes and temperatures as well as biological activities are yet to be studied [7,10,11]. However, during the synthesis process of azo compound, an intramolecular proton transfer between the azo nitrogen atom and hydroxyl oxygen atoms may result in a tautomer hydrazone structure, if both groups feature a para/ortho substitution pattern. This hydrazone tautomer has been studied using various techniques, including UV-VIS and NMR spectroscopy and computational simulations [9,12]. In fact, proton tautomerism plays an important role in many branches of chemistry, particularly biochemistry [9,13]. They can be used as a potential chelating ligand for the synthesis of metal complexes of different geometry which leading to a remarkable property profile and potential uses such like optical signal processing, molecular data processing, ion sensors and biological applications [4].

\* Corresponding author:

sopbue@yahoo.fr (Emmanuel F. Sopbué)

Received: Jul. 26, 2023; Accepted: Aug. 17, 2023; Published: Aug. 28, 2023

Published online at <http://journal.sapub.org/chemistry>

According to the fact that, a metal complex sometimes exhibits better biological activity than the corresponding ligand, many researches focused their work on the synthesis of new metal complexes. To mention a few examples, a cadmium complex with 4-(2-pyridyl azo)-resorcinol, is used as an anti-tumor drug [11], whereas Co (II) and Cu (II) azo-naphthol chelate complexes give a good antibacterial activity [8,11,14]. These previous findings motivated us to embark on the synthesis, characterization of some transition metal complexes and the evaluation of the antibacterial activities of both the ligand and the metals complexes in organic solvents of different polarities, and at different temperatures. The coordination behavior of these hydrazone ligands towards copper (II), cobalt (II) and bismuth (III) ions will also be investigated using different analytical tools. Finally, the antimicrobial effects of these compounds on Gram-positive and Gram-negative bacteria will be explored.

## 2. Experimental Section

### 2.1. Material and General Manipulations

All the reagents and solvents were purchased from Sigma-Aldrich and Fluka and they were used without further purification. The reaction end and the purity of the compounds was determined using thin layer chromatography (TLC plates coated silica gel 60 F254) in a mixture of solvent like ethyl acetate and hexane (10:90, v/v). Visualization was achieved either by UV light (254 nm) or iodine after elution. The melting points of synthesized compounds were determined using a STUART SCIENTIFIC Melting Point Apparatus Model SMP20. Elemental analysis was carried out with Euro EA 3000 from Hekatech GmbH, Friedrich-List-Allee 26, 41844 Wegberg. Infrared spectra were recorded on a Bruker Alpha spectrophotometer (FT-IR Bruker Optik GmbH, Rudolf-Plank-Str. 27, 76275 Ettlingen) using ATR (Attenuated Total Reflectance) technique on a diamond crystal. The UV-visible absorption spectra were recorded using a UNICAM UV 300 spectrophotometers with a quartz cell of an optical path length of 1 cm. The UV-spectra were recorded in the range from 200 to 1000 nm. The ESI positive spectra mass were recorded on a Compact BRUKER spectrometer with a DIONEX Ultimate 3000 brand LC chain. Nuclear magnetic resonance (NMR) experiments (1D and 2D) were performed in DMSO-*d*<sub>6</sub> and MeOH-*d*<sub>4</sub>/CDCl<sub>3</sub> on a 400 MHz JEOL ECZ spectrometer equipped with 5-mm digital auto tune Royal probe (JEOL USA, Peabody, MA). <sup>1</sup>H-NMR spectral data were recorded at 400 MHz while <sup>13</sup>C-NMR data were measured at 100 MHz both with TMS used as internal reference. Powder XRD data was collected on a STOE Stadi-p X-ray powder diffractometer (STOE & Cie GmbH, Darmstadt, Germany) with Cu K $\alpha$ 1 radiation ( $\lambda = 1.54056 \text{ \AA}$ ; Ge monochromator; flat samples) in transmission geometry with a DECTRIS® MYTHEN 1K detector (DECTRIS, Baden-Daettwil, Switzerland). Elemental analyses were performed with a

Euro Vector CHNS-O element analyzer (Euro EA 3000) or a vario MICRO Cube (Co. Elementa Analyzer system). Theoretical calculations were performed with Gaussian 9 software in a B3LYP/6-311G mode. Sonochemical reaction was carried out in an ultrasonic vessel (45 kHz, 80 W). The antibacterial activities were performed using the microdilution method and then the minimal concentration inhibition was determined to evaluate the activity of compounds studied.

### 2.2. Synthesis of (Z)-1-(2-Phenylhydrazono) Naphthalen-2(1H)-one (5)

The azo-naphthol tautomer ligand (L) with the structure depicted in scheme 1 was prepared using the known coupling methods [8,11]. In particular, DMSO-solutions of aniline (1.82 g, i. e. 20 mmol in 5 ml) and of sodium nitrite (1.5 g, i. e. 21.5 mmol in 7 ml) were prepared. Both solutions were thoroughly mixed in an Erlenmeyer flask and placed into a salted ice bath to achieve a temperature range between 0 and 5°C. Under continuous stirring 1.7 ml of concentrated hydrochloric acid is added in small portions; to complete the formation of the diazonium salt stirring continues for about 1 hour. Subsequently 2.88 g (20 mmol) of  $\beta$ -naphthol are dissolved in a 10% sodium hydroxide solution and then gradually added to the cooled aniline diazonium chloride salt. The resulting mixture was continually stirred at 0–5°C for 2 h to complete the reaction. The reaction medium is poured into 250 ml of ice water until the formation of a precipitate can be observed. The precipitate is recovered by filtration and washed with cold and hot water and further purified by recrystallization with ethanol. This procedure leads to a product which, when dried at ambient temperature, gives 3.17 g (yield 75%, m.p. 130.6-131.9°C) of a dark red powder; IR (ATR)  $\nu_{\max}$  (cm<sup>-1</sup>): 3038 (N-H---O), 1619 (C=O---H), 1597 (C=C), 1555 (C=N), 1208 (C-N), 1140 (N-N); UV-visible (ethanol)  $\lambda_{\max}$  (nm) 483-560 (CT), 421, 311 ( $\pi \rightarrow \pi^*$ ); 230 ( $\pi \rightarrow \pi^*$ ); <sup>1</sup>H-NMR (methanol-*d*<sub>4</sub>/CDCl<sub>3</sub>, 400 MHz)  $\delta_{\text{H}}$ : 8.39 (1H, d, *J* = 8 Hz, H-8), 7.61 (1H, d, *J* = 9.6 Hz, H-4), 7.60 (2H, d, *J* = 8.4 Hz, H-2'/H-6'), 7.50-7.48 (1H, m; H-5), 7.47 (1H, m, H-7), 7.39 (2H, m, H-3'/H-5'), 7.29 (1H, m, H-6), 7.21 (1H, m, H-4'), 6.69 (1H, d, *J* = 9.6 Hz, H-3), estimated 16 ppm (NH, not experimentally accessible); <sup>13</sup>C-NMR (methanol-*d*<sub>4</sub>/CDCl<sub>3</sub>, 100 MHz)  $\delta_{\text{C}}$ : 173.5 (1C, C-2), 143.9 (1C, C-1'), 141.0 (1C, C-4), 133.5 (1C, C-8a), 129.9 (1C, C-1), 129.6 (2C, C-3'/C-5'), 129.0 (1C, C-7), 128.7 (1C, C-5), 128.0 (1C, C-4a), 127.3 (1C, C-4'), 125.9 (1C, C-6), 124.8 (1C, C-3), 121.6 (1C, C-8), 118.1 (2C, C-2'/C-6'). (HRESI+): protonated molecular ion [M+H]<sup>+</sup> *m/z* 249.1024. Elemental analysis: C<sub>16</sub>H<sub>12</sub>N<sub>2</sub>O Found (calculated): C: 77.38 (77.40); H: 4.89 (4.87); N: 11.20 (11.28).

### 2.3. Synthesis of Metal Complexes

**Synthesis of Copper (II) Complex 6:** 0.25 g (1 mmol) of ligand L (5) was heated with copper chloride (CuCl<sub>2</sub>·2H<sub>2</sub>O) 0.1705 g (1 mmol) under reflux for 6 hours in 15 mL of

acetone. After cooling to room temperature, the homogeneous mixture was poured into cold NaCl solution and then kept for 15 min in an ice bath. The crude precipitate was collected by filtration, washed several times with water and recrystallized in ethanol to give 0.27 g (70%, m.p. > 300°C) of dark blue powder; IR (ATR)  $\nu_{\max}$  (cm<sup>-1</sup>): 3045 (N-H---O), 1615 (C=O---H), 1595 (C=C), 1545 (C=N), 1212 (C-N), 1142 (N-N), 384 (Cu-Cl); 507 (Cu-N) et 559 (Cu-O); UV-visible (ethanol)  $\lambda_{\max}$  (nm), 483-560 (MLCT), 421, 311 ( $\pi \rightarrow \pi^*$ ); 230 ( $\pi \rightarrow \pi^*$ ); <sup>1</sup>H-NMR (DMSO-*d*<sub>6</sub>, 400 MHz)  $\delta_{\text{H}}$ : 8.53 (1H, d, *J* = 8 Hz, H-8), 7.94 (1H, d, *J* = 9.2 Hz, H-4), 7.85 (2H, d, *J* = 8 Hz, H-2'/H-6'), 7.77 (1H, d, *J* = 7.8 Hz; H-5), 7.59 (1H, m, H-7), 7.52 (2H, m, H-3'/H-5'), 7.44 (1H, m, H-6), 7.36 (1H, m, H-4'), 6.91 (1H, d, *J* = 9.2 Hz), estimated 16 ppm (NH, not experimentally accessible). <sup>13</sup>C-NMR (DMSO-*d*<sub>6</sub> 100 MHz)  $\delta_{\text{C}}$ : 169.4 (1C, C-2), 145.5 (1C, C-1'), 140.6 (1C, C-4), 133.3 (1C, C-8a), 129.7 (1C, C-1), 130.4 (2C, C-3'/C-5'), 129.5 (1C, C-7), 129.7 (1C; C-5), 128.4 (1C, C-4a), 128.6 (1C, C-4'), 126.4 (1C, C-6), 124.5 (1C, C-3), 121.9 (1C, C-8), 119.5 (2C, C-2'/C-6'). MSES<sup>+</sup>: protonated molecular ion [M+2H]<sup>+</sup> m/z 382.9777. Elemental analysis Cu(L)(Cl)<sub>2</sub> Found (calculated) C: 50.15 (50.21); H: 3.19 (3.16); N: 7.30 (7.32).

**Synthesis of Cobalt (II) Complex 7:** To a warm ethanol solution (10 mL) containing 0.25 g (1 mmol) of ligand **5**, a mixture of 0.2 g (0.5 mmol) of cobalt oxalate dihydrate salt in 5 mL ethanol was gradually added. The resulting red mixture was subjected to ultrasonic stirring for 2 hours. The resulting solution was filtered and the filtrate was left to crystallize at room temperature for about 24 hours. The precipitate formed was collected by filtration, washed several times with ice water and a water/ethanol mixture (50:50; v/v), and dried at room temperature to afford 0.55 g (80%, m.p. 132.3-134.9°C) of compound **7** as brown powder; UV-visible (ethanol)  $\lambda_{\max}$  (nm) 483-560 (MLCT), 421, 311 ( $\pi \rightarrow \pi^*$ ); 230 ( $\pi \rightarrow \pi^*$ ); IR (ATR)  $\nu_{\max}$  (cm<sup>-1</sup>): 3500-3180 (OH, H<sub>2</sub>O), 3045 (N-H), 1616 (C=O), 1597 (C=C), 1550 (C=N), 1144 (N-N), 859 (Co-OH), 505 (Co-O), 419 (Co-N); <sup>1</sup>H-NMR (DMSO-*d*<sub>6</sub>, 400 MHz)  $\delta_{\text{H}}$ : 8.53 (2H, d, *J* = 8 Hz; H-8), 7.93 (2H, d, *J* = 9.2 Hz, H-4), 7.84 (4H, d, *J* = 8 Hz, H-2'/H-6'), 7.76 (2H, d, *J* = 7.6 Hz, H-5), 7.59 (2H, m, H-7), 7.52 (4H, m, H-3'/H-5'), 7.43 (2H, m, H-6), 7.35 (2H, m, H-4'), 6.90 (2H, d, *J* = 9.2 Hz), 4.02 (s, NH), 3.29 (s, H<sub>2</sub>O); <sup>13</sup>C-NMR (DMSO-*d*<sub>6</sub> 100 MHz)  $\delta_{\text{C}}$ : 169.4 (2C, C-2), 145.6 (2C, C-1'), 140.6 (2C, C-4), 133.3 (2C, C-8a), 129.7 (2C, C-1), 130.4 (4C, C-3'/C-5'), 129.7 (1C, C-7), 129.5 (2C, C-5), 128.7 (2C, C-4a), 128.4 (2C, C-4'), 126.4 (2C; C-6), 124.5 (2C, C-3), 121.9 (2C, C-8), 119.5 (4C, C-2'/C-6'). MSES<sup>+</sup>: [M+H]<sup>+</sup> m/z 590.1366. Elemental analysis Co(L)<sub>2</sub>(OH)<sub>2</sub> Found (calculated) C: 64.95 (65.20) H: 4.50 (4.45); N: 9.55 (9.50).

**Synthesis of Bismuth (III) Complex 8:** Bismuth (III) complex **8** was synthesized in analogy to the method described above. A solution of 0.3 g (1 mmol) of BiCl<sub>3</sub> in acetone (3 mL) was added dropwise to a mixture of 0.5 g (2 mmol) of ligand **5** in 5 mL of acetone to obtain 1.05 g

(78%, m.p. 131.6-133.5°C) of a dark black powder; UV-visible (ethanol)  $\lambda_{\max}$  (nm) 483-560 (MLCT), 421, 311 ( $\pi \rightarrow \pi^*$ ); 230 ( $\pi \rightarrow \pi^*$ ); IR (ATR)  $\nu_{\max}$  (cm<sup>-1</sup>): 3045 (N-H), 2920 (C-H), 2852 (Ar-H), 1730, 1616 (C=O), 1552 (C=N), 1212 (C-N) 1136 (N-N), 526 (Bi-O), 376 (Bi-N); <sup>1</sup>H-NMR (methanol-*d*<sub>4</sub>/CDCl<sub>3</sub>, 400 MHz)  $\delta_{\text{H}}$ : 8.49 (4H; d, *J* = 8 Hz; H-8), 7.73 (4H, d, *J* = 9.6 Hz, H-4), 7.69 (8H, d, *J* = 7.6 Hz, H-2'/H-6'), 7.57 (4H, m, H-5), 7.52 (4H, m, H-7), 7.45 (8H, m; H-3'/H-5'), 7.35 (4H, m, H-6), 7.27 (4H, m, H-4'), 6.77 (4H, d, *J* = 9.6 Hz, H-3), 4.33 (s, NH); <sup>13</sup>C-NMR (methanol-*d*<sub>4</sub>/CDCl<sub>3</sub>, 100 MHz)  $\delta_{\text{C}}$ : 196.8, 198.0, 172.8, 173.1 (4C; C-2), 144.3 (4C, C-1'), 140.9 (4C; C-4), 133.5 (4C, C-8a), 129.9 (4C, C-1), 129.6 (8C, C-3'/C-5'), 129.0 (4C, C-7), 128.7 (4C, C-5), 128.1 (4C, C-4a), 127.4 (4C, C-4'), 125.9 (4C, C-6), 124.5 (4C, C-3), 121.6 (4C, C-8), 118.2 (8C, C-2'/C-6'), MSES<sup>+</sup> [M-2Cl+Na]<sup>+</sup> at m/z 1259.3121. Elemental analysis, [BiL<sub>4</sub>](Cl)<sub>3</sub> % Found (Calculated): C: 59.01 (58.75); H: 3.80 (3.70); N: 9.20 (9.32).

## 2.4. Biological Assay

### 2.4.1. Microorganisms

The *in-vitro* antibacterial activity of ligand **5** (L) and their metal complexes (**6**, **7** and **8**) was assayed against three gram-negative (*Escherichia coli*. ATCC 8739, *Salmonella Typhi* ATCC 6539, *Klebsiella pneumoniae* 22) and one Gram-positive (*Staphylococcus aureus* ATCC 25923) bacterial strains by the reported method [15]. All strains are reference ones obtained from the American Type Culture Collection. The bacterial strains were grown at 35°C and maintained on nutrient agar (NA, Conda, Madrid, Spain) and the Minimum inhibitory concentrations (MIC) were determined by the liquid micro-dilution method as described earlier [15,16].

### 2.4.2. Determination of Minimum Inhibitory Concentration (MIC) and Minimum Bactericidal Concentration (MBC)

The minimum inhibitory concentration (MIC) was determined using the established method [16]. Micro titer plates (96 micro wells) were prepared and each well received 85  $\mu$ l of Mueller Hinton Agar and 5  $\mu$ l of inoculum. The ligand (**5**) and its metal complexes **6**, **7**, **8** were made at concentrations of 2 mg/mL in 5% (v/v) aqueous solution of dimethylsulfoxide (DMSO) at 5% (v/v). One plate was used for each group of microorganisms. The positive control contained the appropriate medium and the microbial suspension only, whereas negative control was done with an aqueous solution of DMSO or 10% Tween 20 instead of the inoculum. 10  $\mu$ l of each tested compound were prepared and added in subsequently to give a final volume of 100  $\mu$ l. The plates were covered and incubated with shaking at 35°C for 24 hours. Microbial growth was determined by introducing 5  $\mu$ l of a 2 mg/ml para-iodonitrotetrazolium solution. Any color change from yellow to purple indicates microbial growth. The minimum inhibitory concentration has been

defined as the smallest concentration of an antibiotic or substance that prevents this color change. 10  $\mu$ l of the contents of each well were withdrawn aseptically and spread separately on the surface of the medium of Muller Hinton Agar in order to determine the minimum bactericidal concentration (MBC) which is defined as being the smallest concentration giving a sub-negative culture or only one colony. Three replicates were performed for each sample; ciprofloxacin was used as reference drug.

### 3. Results and Discussion

#### 3.1. Chemistry

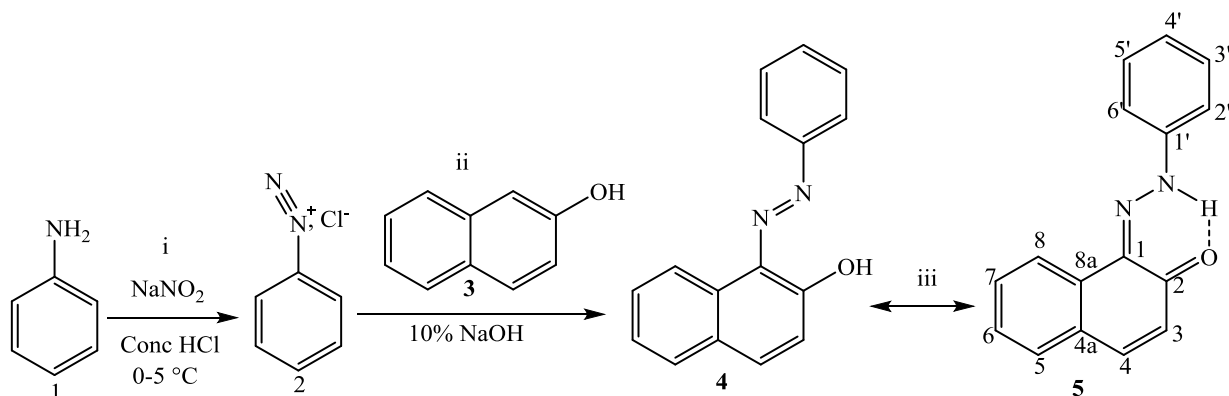
The reaction of (Z)-1-(2-phenylhydrazono) naphthalen-2(1H)-one ligand (L) with the metal ions Cu (II), Co (II), Bi (III), gave different colored powder, depending on the nature of metal ion. The metal complexes were air-stable, insoluble in water, but soluble in some common organic solvents.

**Table 1.** The UV-VIS, physical and analytical data of the ligands and their complexes

Chemical formula	Mass (g/mol)	M.P (°C)	Analysis Found (calculated)			UV-Vis	
			%C	%H	%N	$\lambda_{\max}$ (nm)	
$C_{16}H_{12}N_2O : L$ <b>5</b>	248.095	130.6-131.9	77.38 (77.40)	4.89 (4.87)	11.20 (11.28)	230 311 419-560	$\pi \rightarrow \pi^*$ $\pi \rightarrow \pi^*$ MLCT
$[Cu(L)(Cl)_2]$ <b>6</b>	380.962	> 300	50.15 (50.21)	3.19 (3.16)	7.30 (7.32)	230 311 419-560	$\pi \rightarrow \pi^*$ $\pi \rightarrow \pi^*$ MLCT
$[Co(L)_2(HO)_2]$ <b>7</b>	589.129	132.3-134.9	64.95 (65.20)	4.50 (4.45)	9.55 (9.50)	230 311 419-560	$\pi \rightarrow \pi^*$ $\pi \rightarrow \pi^*$ MLCT
$[BiL_4].Cl_3$ <b>8</b>	1306.267	131.6-133.5	59.95 (58.75)	3.98 (3.70)	8.20 (8.56)	230 311 419-560	$\pi \rightarrow \pi^*$ $\pi \rightarrow \pi^*$ MLCT

**Table 2.** IR frequencies (in  $cm^{-1}$ ) of the ligand and its metal complexes

Compounds	$\nu(O-H)$	N-H	C=O chelated	C=N	C-N	N-N	M-OH	M-O	M-N	M-Cl
Ligand L <b>5</b>	-	3038	1619	1555	1208	1140	-	-	-	-
$[Cu(L)(Cl)_2]$ <b>6</b>	-	3045	1615	1545	1212	1142	-	559	507	384
$[Co(L)_2(HO)_2]$ <b>7</b>	3500-3180	3045	1616	1550	1210	1144	859	505	419	-
$[BiL_4].Cl_3$ <b>8</b>	-	3045	1616, 1730	1552	1212	1136	-	526	376	-



I = diazotization, ii = coupling reaction, iii = tautomer azo (4) and hydrazone (5) form

**Scheme 1.** Reactions' sequences to ligand 5

The synthesized ligand and their metals complexes were characterized by various analytical techniques such as spectroscopy (IR, 1D & 2D NMR, UV-Vis), ESI-mass spectrometric and elemental analysis. The synthesis reaction of the ligand and its metals complexes is depicted in schemes 1 and 2. Physical and analytical analysis are given in table 1, whereas the IR spectroscopy of a ligand and their metal complexes are given in table 2.  $^1\text{H}$ - &  $^{13}\text{C}$ -NMR data are show in table 3. The antibacterial activity of ligand and their metals complexes are listed in table 4.

**UV-Visible:** UV-vis spectrum of the ligand showed three absorption bands between 200 and 570 nm with a shoulder at 421 nm. Indeed, the intense band at 230 nm is attributed to the  $\pi \rightarrow \pi^*$  transition of the moderate energy of the aromatic nucleus ( $^1\text{L}_a$ - $^1\text{A}$ ). The second one at 311 nm is due to the low energy  $\pi \rightarrow \pi^*$  transition of the state ( $^1\text{L}_b$ - $^1\text{A}$ ) [17]. The broad band observed between 450-560 nm can be attributed to an intramolecular charge transfer (CT) interaction involving the entire ketone tautomer molecule [18]. Therefore, the large width of this band may be due to the existence of an equilibrium state between to the azo-hydrazone tautomer originating from the OH group in the ortho position to the azo group N=N [19]. Moreover, the strong intensity of this band proves an absolute dominance of the hydrazone tautomer having established the hydrogen bonds (scheme 1) [20]. On the other hand, the more intense appearance of the band at 230 nm is due to the remarkable aromaticity of one of the cycles caused by the  $\pi$ -donor effect of the OH substituent in the ortho position [19]. The absorption peak of ligand at 311 nm ( $\pi \rightarrow \pi^*$ , transition), 421 nm ( $\pi \rightarrow \pi^*$ , transition) and the broad one between 450-560 nm (CT, electrons) has considerably decreased in all metal complexes. This observation indicates that metals ions are mainly complexed with the ligand through a non-bonding electron pair of the oxygen atom belonging to the ketone and imine groups [10]. Indeed, the coordination of the ligand to the metal creates a charge transfer between the ligand and the metal (MLCT). In case of a MLCT, the geometry of hybrid orbitals occupied determines if a d-d transition can be observed or not [21].

**IR Spectroscopy:** Infrared spectroscopy is an important tool used in coordination chemistry to provide the different functional groups of ligands involved in coordination. The most relevant IR absorption bands corresponding to the ligand and its metals complexes are compiled in table 2. FT-IR of ligand **5** showed one imino band (NH) at  $3038\text{ cm}^{-1}$  and one carbonyl (C=O) band at  $1619\text{ cm}^{-1}$ . However, the FT-IR spectra of this compound lacks the broad band typically for the presence of a hydroxyl group (OH). This suggests that the ligand is present predominantly in keto form in the solid state [4]. If not involved in a hydrogen bond the imino group's N-H-bond typically shows an absorption at  $3400\text{ cm}^{-1}$ , the lower wavenumbers observed for the N-H and the C=O suggest the presence of a hydrogen bond [22]. This finding further supports the hypothesis that the hydrazone tautomer is predominant. Three strong bands at  $1555$ ,  $1208$  and  $1140\text{ cm}^{-1}$  in the ligand are assigned to a C=N, C-N and N-N stretch respectively [22,23].

FT-IR spectra of all metal complexes displayed bands in the same region as a ligand. Nevertheless, slight variations of some band's vibration as well as new absorptions can be observed, probably due to the complexation. In the Cu(II) complex **6** a slight shift of imino and ketone group ( $\Delta\nu = -5\text{ cm}^{-1}$ ) can be observed. This finding may be explained either by the fact that the intramolecular hydrogen bonding remains unaffected by coordination of N-H group or by the neutral nature of the ligand [22,24]. In the Co(II) complex **7**, a new broad band is found, which is caused by the coordination of the water molecule [25]. This assumption is further supported by the appearance of a new band at  $859\text{ cm}^{-1}$ , which is attributed to M-OH. In the IR spectra of the Bi(III) complex **8**, new bands appeared at  $1729\text{ cm}^{-1}$  and  $2920$ - $2850\text{ cm}^{-1}$ . These signals are attributed to a carbonyl group (C=O) group and an aromatic C-H vibration, indicating that in case of Bi(III) the ligands are coordinated in a different way. In addition, the IR spectrum of the ligand showed a stretching vibration signal at  $1140\text{ cm}^{-1}$  assigned to N-N band. When bonded in metals complexes a bathochromic shift of the N-N band to a region between  $1145$  and  $1135\text{ cm}^{-1}$  can be observed indicating the bonding of ligand to the metal ions through imine group. The hypothesis that coordination occurs via the C-N nitrogen is further supported by the variation of C-N frequency band due to the increase in the bond strength. It is worthwhile mentioning that the IR spectra of the complexes exhibited new bands in the range of  $350$ - $600\text{ cm}^{-1}$ . In case of the copper (II) complex these appeared at  $559$ ,  $507$  and  $384\text{ cm}^{-1}$  and can be assigned to Cu-O, Cu-N and Cu-Cl-bonds, respectively. In cobalt (II) complex the bands at  $505$ ,  $419\text{ cm}^{-1}$  were assigned to Co-O and Co-N bonds respectively, whereas in the Bi (III) complex the Bi-O and Bi-N bonds can be found at  $526$  and  $376\text{ cm}^{-1}$ , respectively [26,27]. In consequence, it is reasonable to assume that, the ligand coordinated as a bidentate one by the ketone and imino groups.

#### $^1\text{H}$ and $^{13}\text{C}$ -NMR

The proton and carbon NMR spectra of the complexes resemble that of the free ligand in terms of signal number (9 signals for proton and 14 signals for carbon). In the case of the free ligand the proton signal of OH---N bond was not observed in the usual region around 12 ppm but it experienced a downfield shift to approximately 16 ppm. This deshielding can be attributed to the dominance of the hydrazone tautomer in the free ligand. In case of the Co(II) and Bi(III) complexes, however, the proton of the OH---N bond experienced a significant shift to the upfield region of the spectrum.

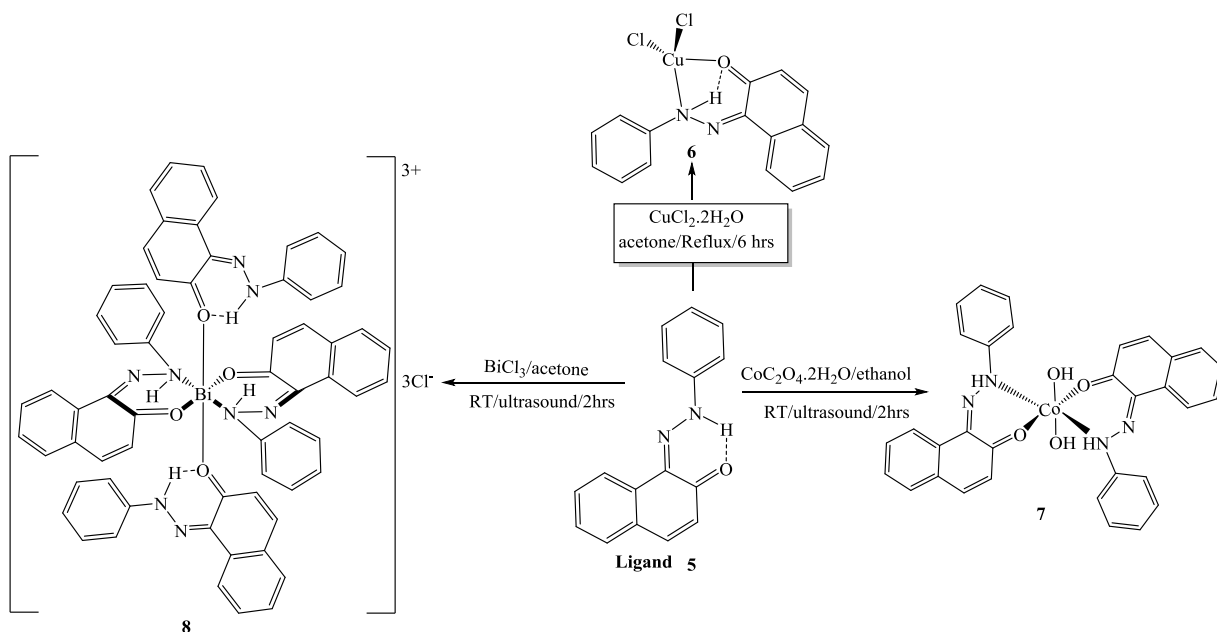
In both complexes it appeared as a singlet at 4.02 ppm (Co(II) complex) and 4.33 ppm (Bi(III) complex); in both cases indicative of the presence of an N-H-bond. Contrary to the two aforementioned complexes in case of the Cu(II) one a signal of the OH---N group was not observed, indicating the presence of a strong hydrogen bond in the complex. Moreover, all the remaining protons of the free ligand as well as of the associated complexes appeared well resolved in the aromatic zone of 6.68-8.60 ppm in the  $^1\text{H}$ -NMR. Protons

closest to the coordination site are more affected by the chelation effect that creates a delocalization of the  $\pi$ -electrons in the aromatic ring: in the metals complexes the protons H-3, H-4 and H-2'/H-6', which appeared in the ligand at 6.69, 7.61 and 7.60 ppm, respectively, were shifted downfield to a region of 7.69-7.95 ppm, indicating the involvement of the ketone and imino group in coordination. In the case of the Co(II) complex the  $^1\text{H-NMR}$  signal

observed at 3.29 ppm is caused by hydroxyl group directly attached to cobalt ion. To confirm the structures of the complexes shown in scheme 2, relative intensities of the integral values of each proton were determined to calculate the metal ligand coordination ratio. This procedure lead to ratios of 1:1, 1:2, and 1:4 for complexes 6, 7 and 8 respectively, in full agreement with the proposed structure of the complexes presented in scheme 2.

**Table 3.** Comparison of the  $^1\text{H}$  and  $^{13}\text{C-NMR}$  chemical shifts ( $\delta_{\text{H}}$  and  $\delta_{\text{C}}$  in ppm) ligand **5** and those of the metal complexes **6**, **7** and **8**

N° C/H	L		Metals complexes					
	<b>5</b>		[Cu(L)(Cl) <sub>2</sub> ] <b>6</b>		[Co(L) <sub>2</sub> (HO) <sub>2</sub> ] <b>7</b>		[BiL <sub>4</sub> ].Cl <sub>3</sub> <b>8</b>	
1	129.9	-	129.7	-	129.7	-	129.9	-
2	173.5	-	169.4	-	169.4	-	196.8,	172.8,
							198.0,	173.1
3	124.8	6.69 (1H)	124.5	6.91 (1H)	124.5	6.90	124.5	6.77 (4H)
4	141.0	7.61 (1H)	140.6	7.94 (1H)	140.6	7.93	140.9	7.73 (4H)
4a	128.0	-	128.4	-	128.7	-	128.1	-
5	128.7	7.50-7.48(1H)	129.7	7.77 (1H)	129.5	7.76 (2H)	128.7	7.57 (4H)
6	125.9	7.29 (1H)	126.4	7.44 (1H)	126.4	7.43 (2H)	125.9	7.35 (4H)
7	129.0	7.47 (1H)	129.5	7.59 (1H)	129.7	7.59 (2H)	129.0	7.52 (4H)
8	121.6	8.39 (1H)	121.9	8.53 (1H)	121.9	8.53 (2H)	121.6	8.49 (4H)
8a	133.5	-	133.3	-	133.3	-	133.6	-
1'	143.9	-	145.5	-	145.6	-	144.3	-
2'/6'	118.1	7.60 (2H)	119.5	7.85(2H)	119.5	7.84 (4H)	118.2	7.69 (8H)
3'/5'	129.6	7.39 (2H)	130.4	7.52 (2H)	130.4	7.52 (4H)	129.6	7.45 (8H)
4'	127.3	7.21 (1H)	128.6	7.36 (1H)	128.4	7.35 (2H)	127.4	7.27 (4H)
N-H	-	-	-	-	-	4.02	-	4.33
HO	-	-	-	-	-	3.29	-	-



**Scheme 2.** Reactions sequences to the metal complexes **6**, **7** and **8**

The  $^{13}\text{C}$ -NMR spectra of the ligand and its metals complexes were in perfect agreement with all the informations previously observed. Indeed, an upfield shift of the ketone carbonyl carbon and of the C-N imine carbon of  $\Delta\delta_c = 4.1$  and 1.7 ppm, respectively, are observed in all the complexes confirming the bidentate coordination of the ligand to the central metal via the carbonyl and the nitrogen of the C-N group.

Moreover, the absence of signals from the carbonyl of the oxalate showed that the oxalate ion was not bonded to the central metal. The assignments of the various proton and carbon signals observed are compiled in table 3. It should be stressed that in the Bi(III) complex additional signals at 198.0, 196.8, 173.1, and 173.0 ppm were found, indicating slight variations in the carbonyl group's coordination to the Bi(III) ion.

### XRD Patterns of metals complexes:

X-ray powder diffractions were performed for the ligand and their metals complexes, and comparative diffractogram results are given on figure 1. The diffractograms of complexes **6** and **8** differ from each other as well as from the pattern of the ligand **5**.

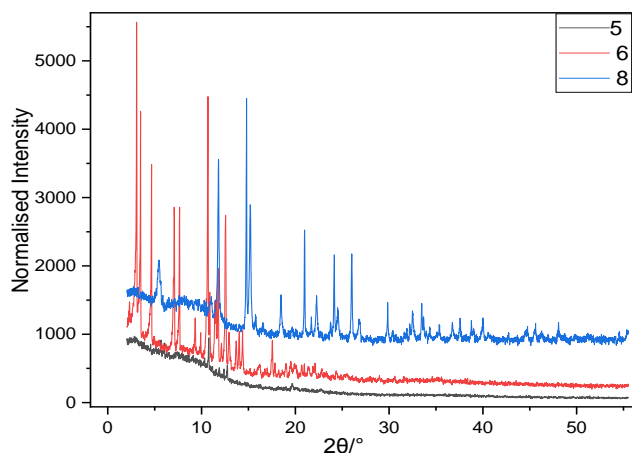


Figure 1. XRPD Patterns of the ligand (**5**) and of complexes **6** and **8**

However, in contrary to the ligand's XRD, which does not show distinctive signals, metals complexes **6** and **8** exhibit many well resolved peaks due to their crystalline structure. According to the previous study on bismuth complex [26,28,30,31], we suggest that in compound  $[\text{BiL}_4]\cdot\text{Cl}_3$  (**8**), the bismuth atom exhibits a six-fold coordination in which two ligands are coordinated to a central atom ion in a bidentate pattern, whereas the two remaining ligands are monodentate ones coordinated through carbonyl group (scheme 2).

### 3.2. Biology

The antibacterial effects of ligand **5** and its metals complexes **6**, **7** and **8** against gram-positive and gram-negative bacteria are compiled in table 4. All the compounds synthesized showed different degrees of antibacterial activity against tested bacterial (MIC = 32-128  $\mu\text{g}/\text{mL}$ ) but did not exceed the activity of the reference drug ciproflocine. Nevertheless, the metals complexes had either the same or a higher activity as the ligand. The copper (II) complex **6** showed an intermediated activity (MIC = 64  $\mu\text{g}/\text{mL}$ ) against *E. coli*, *S. aureus*, *Salmonella Typhi* and the least one (MIC = 128  $\mu\text{g}/\text{mL}$ ) against *Klebsiella pneumoniae*. The cobalt and bismuth complexes **7** and **8** had an intermediated activity (MIC = 64  $\mu\text{g}/\text{mL}$ ) against *E. coli*, and the least one (MIC = 128  $\mu\text{g}/\text{mL}$ ) against *S. aureus* and *Klebsiella pneumoniae*. However, both complexes are significantly more active against *Salmonella Typhi* (MIC = 32  $\mu\text{g}/\text{mL}$ ) than the free ligand. Based on MBC and MBC/MIC results in table 4, all metal complexes and ligand had a bacteriostatic effect (MBC/MIC = 2) against the tested bacterial strains, except the copper complex which had an absolute bactericidal effect (MBC/MIC = 1) against *Klebsiella pneumoniae*. Presumably, the structural factors which govern antimicrobial activities are strongly dependent on the central metal ion [29]. The difference activity between ligand and their metals complexes are since described basis of overtone's concept of cell permeability.

Table 4. Antibacterial Activity (MIC and MBC in  $\mu\text{g}/\text{mL}$ ) of ligand and metal complexes

Microorganisms	Inhibition	Ligand	Metals complexes parameters				Reference drug
		<b>5</b>	<b>6</b>	<b>7</b>	<b>8</b>		
<i>E. coli</i> ATCC 8739	MIC	64	64	64	64	4	
	MBC	128	128	128	128	4	
	MBC/MIC	2	2	2	2	1	
<i>S. aureus</i> ATCC 25923	MIC	128	64	128	128	2	
	MBC	256	128	256	256	4	
	MBC/MIC	2	2	2	2	2	
<i>Salmonella Typhi</i> ATCC 6539	MIC	128	64	32	32	2	
	MBC	256	128	64	64	4	
	MBC/MIC	2	2	2	2	2	
<i>Klebsiella pneumoniae</i> 22	MIC	128	128	128	128	2	
	MBC	256	128	256	256	4	
	MBC/MIC	2	1	2	2	2	

Based on this concept, chelation is certainly responsible for the enhanced activities shown by the metals complexes. In fact, the polarity of the metal ion will be reduced to greater extent on chelation, due to the overlap of the ligand orbital and partial sharing of the positive charge of the metal ion with donor groups [28]. Then, the lipid membrane that surrounds the cell favors the passage of lipid soluble materials due to its liposolubility [28]. Moreover, an increased activity indicates enhances in the lipophilicity of the complexes due to the delocalization of  $\pi$ -electrons in the chelated ring thus leading to the breakdown of the permeability barrier of the cell [11]. This process promotes the penetration of the complex into the lipid membrane of the microorganism to aggressively destroy the latter by blocking the enzymatic process or by disturbing its respiration process during protein synthesis, thus preventing its growth [32].

### 3.3. HOMO-LUMO Analysis and Molecular Electrostatic Potential (MEP)

Computational methods are very important in chemistry as they allow a prediction of many chemical properties as well as polarizability, chemical reactivity and kinetic stability of the molecule synthesized. Therefore, the energy band gap (HOMO-LUMO) and the global reactivity descriptors of the ligand and its metals complexes are evaluated using hybrid functional B3LYP and triple zeta basis set with both diffuse functions, 6-311++G (d, p) [33]. The calculations indicate that the ligand **5** has 65 occupied molecular orbitals and the value of the energy separation between the LUMO and HOMO is 2.999 eV. Therefore, in order to identify the electrophilic and nucleophilic regions, Molecular Electrostatic Potential (MEP) was computed for an optimized structure and the results are given in figure 2. The red color specifies the higher negative potential regions which are beneficial for electrophilic attack, whereas the blue color identifies the higher positive potential regions favorable for nucleophilic attack.

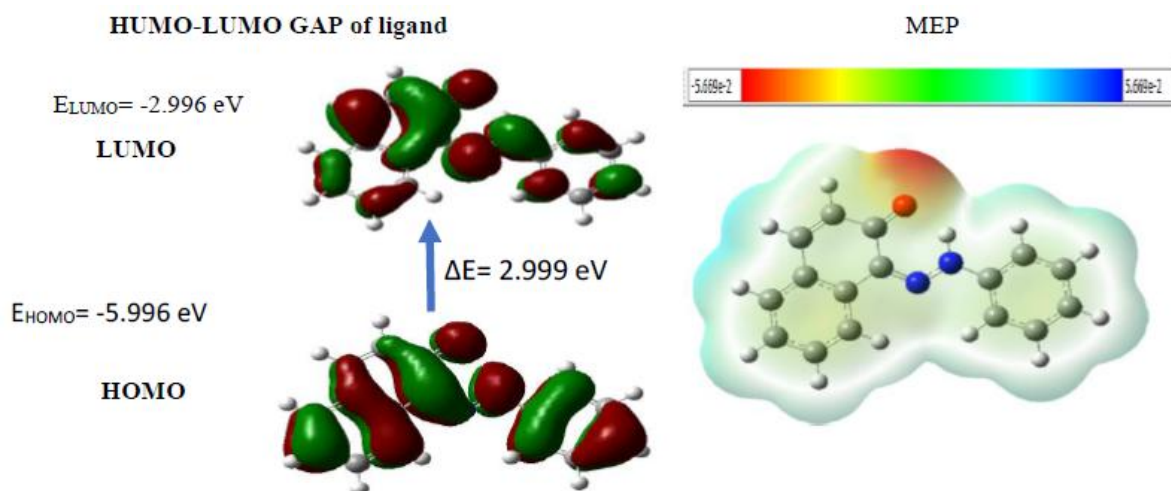


Figure 2. Structures of the FMO (HOMO and LUMO) and MEP of Compound 5

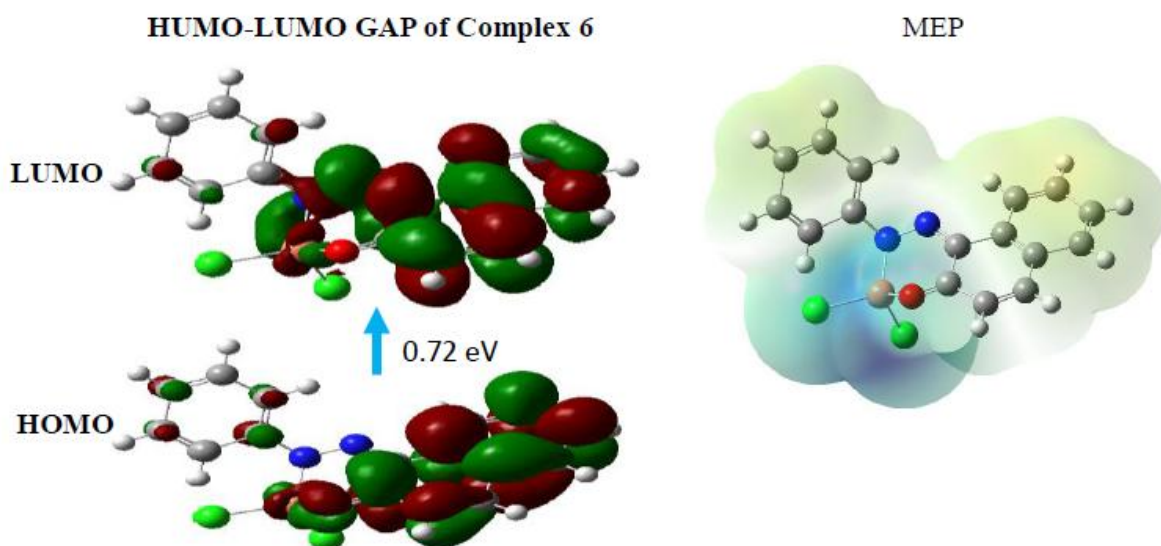


Figure 3. Structures of the FMO (HOMO and LUMO) and MEP of compound 6

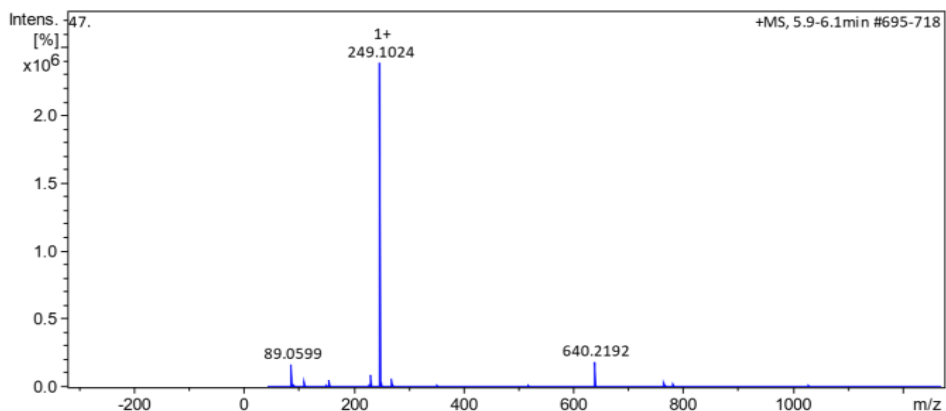


Figure 4a. HRESI+ mass spectrum of ligand 5

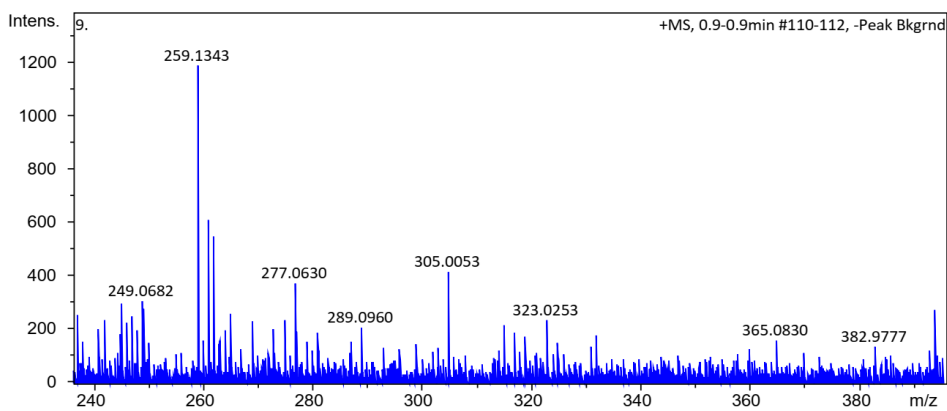


Figure 4b. HRESI+ mass spectrum of complex 6

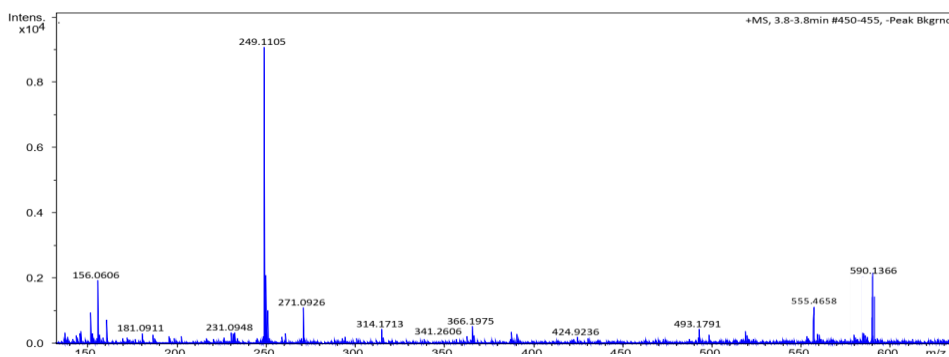


Figure 4c. HRESI+ mass spectrum of complex 7

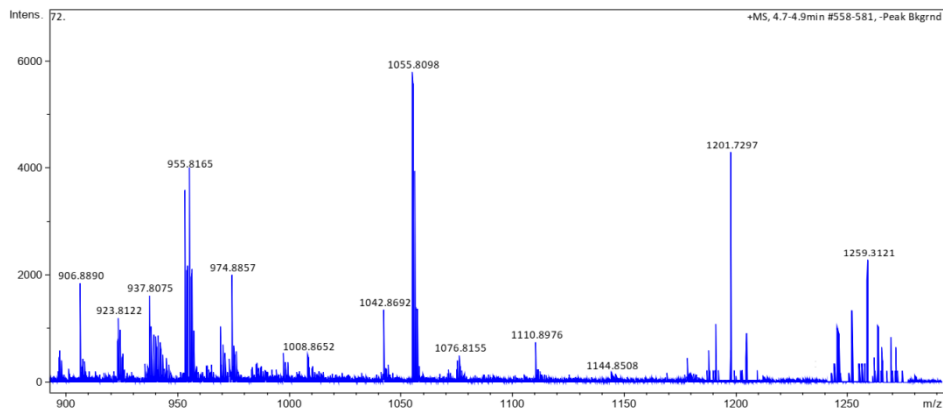


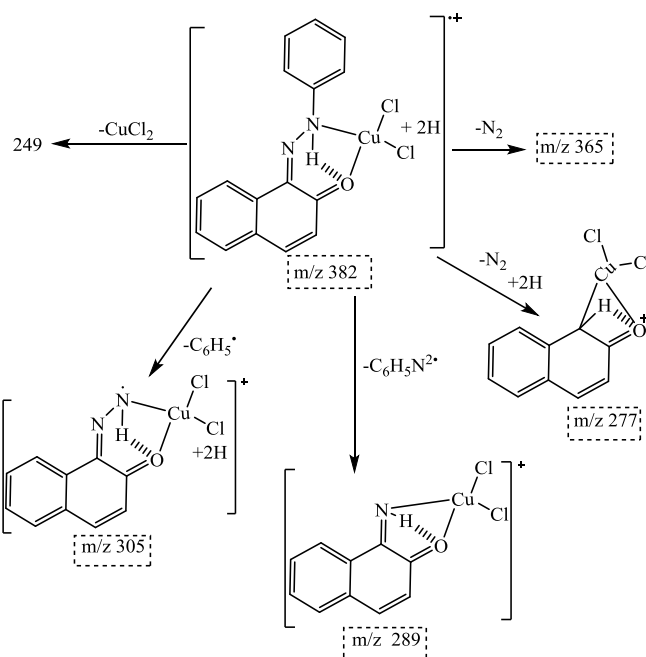
Figure 4d. HRESI+ mass spectrum of complex 8

As can be seen from the figure, there is one possible site on the ligand for electrophilic attack. These negative regions are localized on the oxygen atoms with maximum value of -5,669 a. u. Their involvement in coordination site leads to the loss of their nucleophilic proprieties. In order to justify this hypothesis, the structure of complex **6** was further optimized in terms of energy. MEP results are outlined in figure 3.

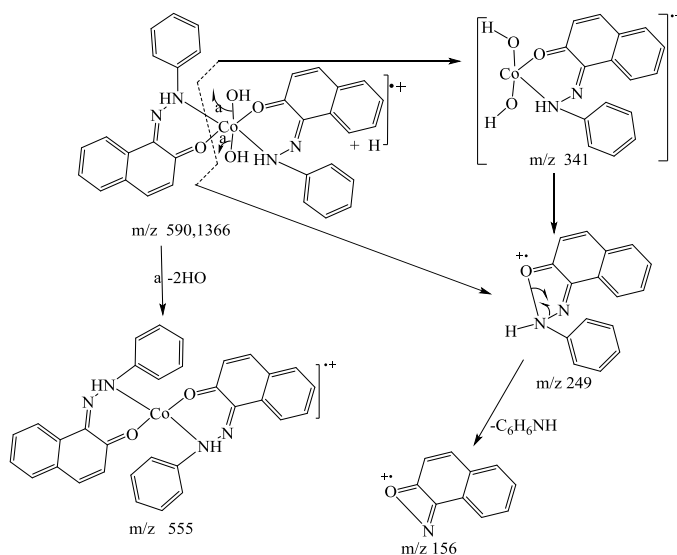
#### 4. Mass Spectrum and Fragmentations' Patterns of the Compounds

HRESI+ mass spectrum of ligand and their metal complexes are presented in figure 4 (4a, 4b, 4c, 4d).

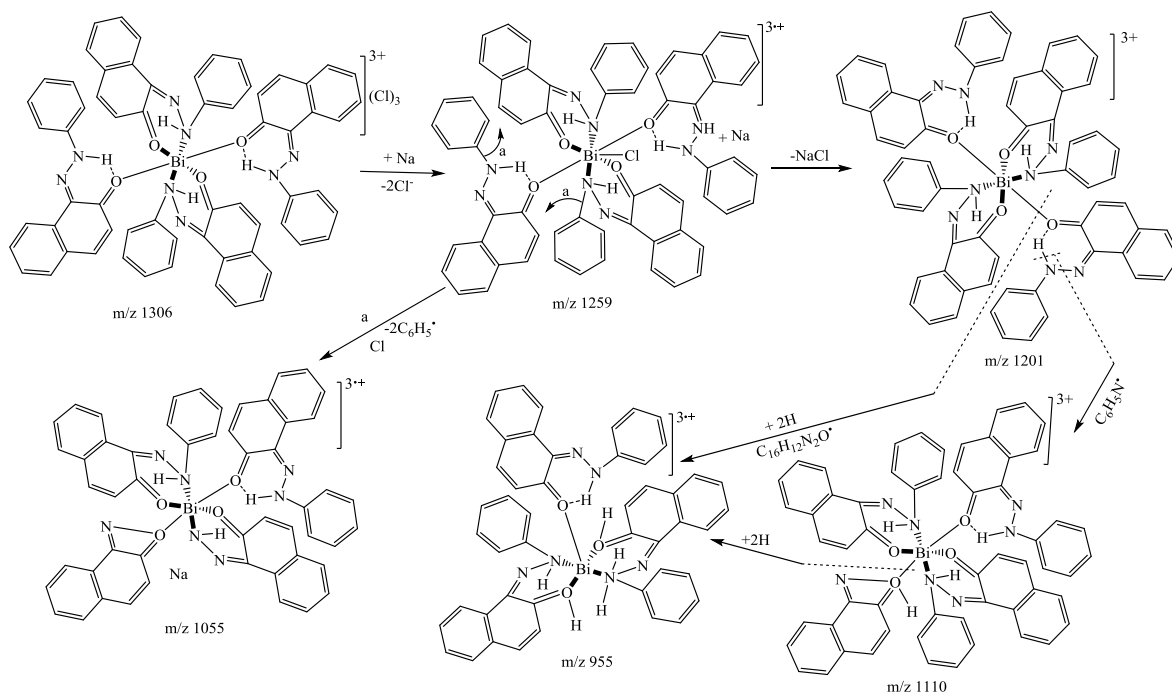
The HRESI+ Mass spectrum of the ligand displayed a molecular protonated ion  $[M + H]^+$  at  $m/z$  249.1024 in good agreement with proposed formula **5**. In addition, the proposed formula of metal complexes are well confirmed by different molecular ions in their spectra as well as  $[M + 2H]^+$  at  $m/z$  382.9777,  $[M + H]^+$  at  $m/z$  590.1366 for Cu (II) **6** and Co (II) **7** complexes respectively. It may happen during an ESI mass analysis of a complex, that the counter ions are bonded to a central metal atom and reduce the total charge of the complex fragment ion [34]. That is while in Bi(III) complex **8** spectrum, molecular ion are not observed but, the ion-fragment  $[M - 2Cl + Na]^+$  is observed at  $m/z$  1259.3121. The fragmentation pattern of complexes **6**, **7** and **8** are shown in the schemes 3, 4 and 5 respectively.



Scheme 3. Fragmentation pattern of complex **6**



Scheme 4. Fragmentation pattern of complex **7**



Scheme 5. Fragmentation pattern of complex 8

## 5. Conclusions

The synthesized ligand **5** (*Z*)-1-(2-phenylhydrazono)naphthalen-2(1*H*)-one acts as a bidentate ligand. The IR, NMR (1D & 2D), ESI+ Mass spectrum and electronic studies confirm that the ligand coordinated to metal through oxygen and nitrogen as donor atoms. This ligand is used to synthesize copper (II), cobalt (II) and bismuth (III) complexes. The results of this investigation support the suggested structures of the metal complexes in which the copper (II) complex exhibits a tetrahedral geometry, whereas cobalt (II) and bismuth (III) complexes show an octahedral coordination. *In vitro* antibacterial properties were evaluated against four bacterial strains (three Gram-negative, one Gram-positive). All compounds showed activity against bacteria; however, metal complexes have a higher activity than the non-complexed ligand.

## Conflict of Interests

The authors declare that they have no conflict of interests.

## ACKNOWLEDGMENTS

Emmanuel Sopbué Fondjo warmly thanks the financial support of the DAAD (grant n° 91691265). Additional financial support was obtained from the research grant committee of the University of Dschang and the Cameroonian Higher Education Ministry.

## REFERENCES

- [1] Song, H., Chen, K., Wu, D., & Tian, H., 2004. Synthesis and Absorption Properties of Some new Azo-Metal Chelates and their ligands. *Dyes and Pigments*, 60, 111–119. [doi:10.1016/S0143-7208(03)00144-X]
- [2] Tanaka, K., Matsuo, K., Nakanishi, A., JO, M., Shiota, H., Yamaguchi, M., Kawaguchi, K., 1984. Syntheses and Antimicrobial activities of five-membered Heterocycles Having a Phenylazo Substitute. *Chemical & Pharmaceutical Bulletin*, 32, 3291–3298. [doi:10.1248/cpb.32.3291]
- [3] Fahad, T.A., yaqoob, R.H., 2015. Preparation, Characterization and Antimicrobial activity of New Azo Complexes Containing Paracetamol. *World Journal of Pharmaceutical Research*, 5, 35-43
- [4] Rauf, M.A., Hisaindee, S., & Saleh, N., 2015. Spectroscopic Studies of Keto–Enol Tautomeric Equilibrium of Azo Dyes. *RSC Advances*, 5, 18097–18110. [doi: 10.1039/c4ra16184j]
- [5] Abdallah, S.M., 2010. Metal Complex of Azo Compounds derived from 4-acetamidophenol and Substituted Aniline. *Arabian journal of Chemistry*, 5, 251-256. [doi:10.1016/j.arabjc.2010.08.019]
- [6] Langhals, H. (2004). Color Chemistry. Synthesis, Properties and Applications of Organic Dyes and Pigments. 3<sup>rd</sup> revised edition. By Heinrich Zollinger. *Angewandte Chemie International Edition*, 43(40), 5291–5292. [doi:10.1002/anie.200385122]
- [7] Elisangela F, Andrea Z, Fabio DG, Cristiano RM, Regina DL, Artur CP., 2009. Biodegradation of Textile Azo Dyes by a Facultative Staphylococcus Arlettae Strain VN-11 using a sequential microaerophilic/aerobic process. *International Biodeterioration and Biodegradation*, 63, 280-288. [doi:10.1016/j.ibiod.2008.10.003]

- [8] Vidyaa, V.G et Sadasivana, V. 2023. Synthesis, spectroscopic characterization and biological activities of some metal complexes with new heterocyclic azodye ligand 2-(2- hydroxynaphthalen-1-yl azo) -pyridin-3-ol. *Current Chemistry Letters* 12, 55–64. [doi: 10.5267/j.ccl.2022.9.006]
- [9] Kourosch, H., Mohsen, I., Ezzat, R., and Mohammad J., 2012. Synthesis, Characterization, and Tautomeric Properties of Some Azo-Azomethine Compounds. *Zeitschrift fur Naturforsch*, 67b, 159 – 164. [doi: 10.5560/ZNB.2012.67b0159]
- [10] Abdalla, M. K., Mohamed, G., Raafat, M. I., Hasn, E., 2005. Synthesis and spectral studies of 5-[3-(1,2,4-triazolyl-azo)-2,4- dihydroxybenzaldehyde (TA) and its Schiff bases with 1,3-diaminopropane (TAAP) and 1,6-diaminohexane (TAAH). Their analytical application for spectrophotometric microdetermination of cobalt(II). Application in some radiochemical studies. *Dyes and Pigments* 67 117-126. [doi:10.1016/j.dyepig.2004.11.004]
- [11] Asmaa, A., Al-hassani, Abbas, H., Al-Khafagy, Abid Allah, Ali, M., 2014. Preparation, Characterization and Biological Activity of New Azo Ligand and Some of its Metal Molecules. *World Journal of Pharmaceutical Research*, 3, 218-231.
- [12] Krzysztow, W., Lucjan, S., 2016. [Azo-Hyd] Tautomerism and Structure of Selected Metal Complex Dyes AM1 and ZINDO/1 Methods. *Computational Chemistry*, 4, 97-118 [doi: 10.4236/cc.2016.44010]
- [13] Kirilmis, C., Ahmedzade, M., Servi, S., Koca, M., Kizirgil, A., & Kazaz, C. 2008. Synthesis and Antimicrobial Activity of Some novel derivatives of Benzofuran: Part 2. The Synthesis and Antimicrobial Activity of Some Novel 1-(1-benzofuran-2-yl)-2- mesitylethanone Derivatives. *European Journal of Medicinal Chemistry*, 43, 300–308. [doi:10.1016/j.ejmech.2007.03.023]
- [14] Ibrahim Yahya, W., Tahir Mahdi, R., & Kadhem Al-Hakeim, H., 2019. Synthesis, Spectral Identification and Biological Activity of Chelate Complexes Derived from New Azo Naphthresorcenol. *Journal of Physics: Conference Series*, 1294, 052066. [doi:10.1088/1742-6596/1294/5/052066]
- [15] Tamokou, J.-de-D., Tala, F.M., Wabo, K.H., Kuate, J.R., Tane, P., 2009. Antimicrobial Activities of Extract and Compounds from stem bark of *Vismia rubescens*. *Journal of Ethnopharmacology*, 124, 571–575. [doi:10.1016/j.jep.2009.04.062]
- [16] Tamokou, J.-D.D., Mbaveng, A.T., & Kuete, V., 2017. Antimicrobial Activities of African Medicinal Spices and Vegetables. *Medicinal Spices and Vegetables from Africa*, 207–237. [doi:10.1016/b978-0-12-809286-6.00008-x]
- [17] Nilgün Kabay; Emin Erdem; Rafet Kılınçarslan; Eylem Yıldırım Sarı (2007). *Synthesis and characterization of some o'-dihydroxyazo dyes and their metal complexes.* , 32(8), 1068–1072. [doi:10.1007/s11243-007-0283-6]
- [18] Deneva, V., Burdzhiev, N., Stanoeva, E., & Antonov, L., 2010. Tautocrowns: Aza-15-Crown Moiety Conjugated to a Tautomeric Schiff Base. *Spectroscopy Letters*, 43, 22–27. [doi:10.1080/00387010903260273]
- [19] Khanmohammadi, H., & Darvishpour, M., 2009. New Azo Ligands Containing Azomethine Groups in the Pyridazine-based chain: Synthesis and Characterization. *Dyes and Pigments* 81, 167–173. [doi:10.1016/j.dyepig.2008.07.019]
- [20] Kourosch, H., Mohsen, I., Ezzat, R., and Mohammad, J., 2012. Synthesis, Characterization, and Tautomeric Properties of Some Azo-azomethine Compounds. *Zeitschrift fur Naturforschung* 67b, 159 – 164. [doi: 10.5560/ZNB.2012.67b0159]
- [21] Salimova, I. A., Yudina, A. V., Mironov, A. V., Majouga, A. G., Zyk, N. V., & Beloglazkina, E. K., 2018. A Convenient Synthesis of Copper(II) bis[5-(pyridin-2-yl-methylidene)-2-thiohydantoin] Complexes. *Mendeleev Communications* 28, 524–526. [doi: 10.1016/j.mencom.2018.09.025]
- [22] Souza, P., Garcia-Vazquez, J.A., & Masaguer, J.R., 1985. Synthesis and Characterization of Copper (II) and Nickel (II) Complexes of the Schiff Base Derived from 2-(2-aminophenyl) Benzimidazole and Salicylaldehyde. *Transition Metal Chemistry*, 10, 410–412.
- [23] Nora, H. Al-Shaalan, 2011. Synthesis, Characterization and Biological Activities of Cu(II), Co(II), Mn(II), Fe(II), and UO<sub>2</sub>(VI) Complexes with a New Schiff Base Hydrazone: O-Hydroxyacetophenone-7-chloro-4-quinoline Hydrazone. *Molecules*, 16, 8629-8645. [doi 10.1007/s11243-006-0134-x]
- [24] Masoud, M.S., Khalil, E.A., Hindawy, A.M., Ali, A.E., & Mohamed, E.F., 2004. Spectroscopic Studies on Some Azo Compounds and Their Cobalt, Copper and Nickel Complexes. *Spectrochimica Acta Part A: Molecular and Biomolecular Spectroscopy*, 60, 2807–2817. [doi:10.1016/j.saa.2004.01.019]
- [25] Mesmer, R. E., & Baes, C. F., 1990. Review of Hydrolysis Behavior of Ions in Aqueous Solutions. *MRS Proceedings*, 180, 85–96
- [26] Ming-Xue Li; Li-Zhi Zhang; Min Yang; Jing-Yang Niu; Jing Zhou (2012). Synthesis, crystal structures, in vitro biological evaluation of zinc(II) and bismuth(III) complexes of 2-acetylpyrazine N(4)-phenylthiosemicarbazone. , 22(7), 2418–2423. doi:10.1016/j.bmcl.2012.02.024
- [27] Nakamoto, K., 1978. *Infrared and Raman Spectra of Inorganic and Coordination Compounds*, 3rd ed., John Wiley and Sons: New York, NY, USA 1, 359–368.
- [28] Sopbué, E. F., Siéwé, D. A., Tamokou, J.-de-D., Ekom, S. E., Djeukoua, S. K. D., Doungmo, G., Walters M. E., Tsopmo A., Peter F. W. S., and Kuate, J. R., 2020. Room Temperature Synthesis and Characterization of Novel Bi(III) Complex with 2-Amino-3- Carbomethoxy-4,5,6,7-Tetrahydrobenzo[B ]Thiophene as Potential Antimicrobial Agent. *Acta Chim. Slov* 67, 203–211. [doi: 10.17344/acsi.2019.5365]
- [29] Sopbué, E. F., Kemvou T. R., Siéwé, D. A., Tamokou, J.-de-D., Ekom, S. E., Djeukoua, S. K. D., Doungmo, G., Walters M. E., Tsopmo A., Peter F. W. S., and Kuate, J. R., (2020). Synthesis, Characterization and Antimicrobial Activities of Novel Hg(II) Complex with 3-Amino-1-[2-phenyl diazenyl] -4Hthieno [3,4-c]chromen-4-one. *IOSR Journal of Applied Chemistry* 13, PP 08-15 [doi: 10.9790/5736-1303010815]
- [30] Frutos, A., Sala, L., Escandar, G., Devillers, M., Salas Peregrin, J., & González Sierra, M., 1999. Bismuth(III) complexes of d-gluconic acid. *Studies in Aqueous Solution and in the Solid Phase. Polyhedron*, 18, 989–994. [doi:10.1016/s0277-5387(98)00384-2]
- [31] Ozturk, I. I., Banti, C. N., Kourkoumelis, N., Manos, M. J.,

- Tasiopoulos, A. J., Owczarzak, A. M., Hadjikakou, S. K., 2014. Synthesis, Characterization and Biological Activity of Antimony(III) or Bismuth(III) Chloride Complexes with Dithiocarbamate Ligands Derived from Thiuram Degradation. *Polyhedron*, 67, 89–103. [doi:10.1016/j.poly.2013.08.052]
- [32] Mahalakshmi, N., and Rajavel, R., 2014. “Synthesis, Spectroscopic, DNA Cleavage and Antibacterial Activity of Binuclear Schiff Base Complexes,” *Arabian Journal of Chemistry* 7, 509–517. [doi:10.1016/j.arabjc.2010.11.010]
- [33] Akoun, A., Abdoulaye, D., Amadou, T., I., Olivier, O., Adama, S., 2020. Synthesis, Spectrometric Characterization (ESI-MS, NMR, IRTF), X-Ray Study and Quantum Chemical Calculations of 2-oxo-2H-chromen-7-yl Benzoate *American Journal of Organic Chemistry* 10, 1-16. [doi: 10.5923/j.ajoc.20201001.01]
- [34] Henderson, W., & McIndoe, J. S., 2005. *Mass Spectrometry of Inorganic, Coordination and Organometallic Compounds: Tools-Techniques-Tips*, Chichester, UK: John Wiley & Sons, doi:10.1002/0470014318.